Micromachined array tip for multifocus fiber-based optical coherence tomography

Victor X. D. Yang, Nigel Munce, Julius Pekar, Maggie L. Gordon, and Stewart Lo

Department of Medical Biophysics, University of Toronto, Toronto, Ontario M5G 2M9, Canada

Norman E. Marcon

Division of Gastroenterology, St. Michael's Hospital, Toronto, Ontario M5B 1W8, Canada

Brian C. Wilson and I. Alex Vitkin

Department of Medical Biophysics, University of Toronto, and Ontario Cancer Institute, Toronto, Ontario M5G 2M9, Canada

Received February 24, 2004

High-resolution optical coherence tomography demands a large detector bandwidth and a high numerical aperture for real-time imaging, which is difficult to achieve over a large imaging depth. To resolve these conflicting requirements we propose a novel multifocus fiber-based optical coherence tomography system with a micromachined array tip. We demonstrate the fabrication of a prototype four-channel tip that maintains a 9–14-μm spot diameter with more than 500 μm of imaging depth. Images of a resolution target and a human tooth were obtained with this tip by use of a four-channel cascaded Michelson fiber-optic interferometer, scanned simultaneously at 8 kHz with geometric power distribution across the four channels. © 2004 Optical Society of America

OCIS codes: 170.4500, 170.3880, 170.1650, 060.2350, 220.4000.

Optical coherence tomography[1] (OCT) can be used to collect data from multiple focal spots in parallel through the *en face* imaging mode or a raster scan of a single focal spot throughout the cross-sectional plane. By use of CCD[2] or customized array detectors[3] to acquire two-dimensional *en face* images, the signal bandwidth per focal spot can be maintained in the kilohertz range, since the depth scan is performed at low frequency.[4] The slow depth scanning (<100 Hz) also allows focus tracking by use of bulk optics with a reasonable numerical aperture (NA, >0.1) to achieve good lateral resolution over the entire scanning depth.[5,6] Fusion of multiple cross-sectional images at different focal depths has been employed to obtain ultrahigh-resolution OCT images, demonstrating the benefit of improved signal intensity as well as lateral resolution with a higher NA[7]; however, the images from different depths were not acquired simultaneously, thus increasing the imaging time. Because of component size constraints and incompatibility with fiber optics, such schemes have not been used in endoscopic applications, which typically have a low NA to avoid beam divergence along the scanning axis and use the raster-scan approach with a single focal spot. Previously, Qi *et al.* described a microelectromechanical system membrane mirror system for high-speed (8-kHz) dynamic focus tracking.[8] In this Letter we present an alternative fiber-optic design that provides simultaneous multifocus cross-sectional scanning compatible with endoscopy, which has the added benefits of signal bandwidth reduction and more efficient source power distribution for different imaging depths.

Multiple foci can be formed simultaneously by use of a single lens with several fibers arranged in an appropriate pattern, the simplest of which is a stepped linear array, as shown in Fig. 1(a). We fabricated a prototype array of four single-mode fibers (SMF-28), using a modified UV confocal laser scanning microscope (Carl Zeiss, CLSM 510) with an assembly of six micropositioning stages. Four cleaved single-mode fibers without a buffer ($\varnothing$ = 125 μm) were coated with a high-viscosity optical adhesive (Norland, NOA 68) and positioned in a 125-μm stepped pattern by use of individual micropositioning stages on the microscope. The optical adhesive between the fibers was selectively cured with a software-defined mask scanned by the CLSM with 5 mW of power at 351 nm. The curing process was monitored by the CLSM through a bandpass filter (375–480 nm) while the solidifying adhesive fluoresced under UV excitation, as shown in Fig. 1(b). Excess adhesive was removed with acetone, and the resultant fiber array tip was imaged with scanning electron microscopy, as shown in Fig. 1(c), with the expected beam focal profile in Fig. 1(d).

To characterize the performance of the array tip we attached it to a four-channel cascaded Michelson interferometer constructed from eight 3-dB fiber-optic couplers, as shown in Fig. 2(a). The output power of a broadband source (18 mW with a 63-nm bandwidth centered at 1.3 μm) was split into a geometric series, as shown in Fig. 2(b), at the light source input end of each level of the cascade, and the stronger channels were used to scan greater depths. Each of the sample arms contained different lengths of fiber loops, which ensured that no coherent cross talk can occur between channels. The reference arms were connected to a 4 × 1 coupler and shared a common rapid-scanning optical delay (RSOD) line operating sinusoidally at 8 kHz with the images acquired during

0146-9592/04/151754-03$15.00/0

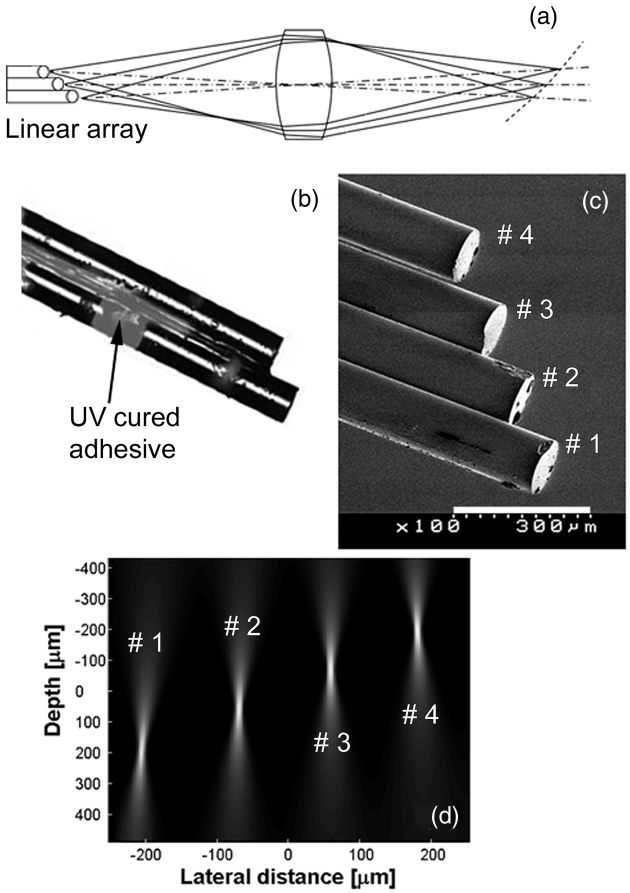

Fig. 1. (a) Schematic for forming multiple foci by use of a linear fiber array. (b) CLSM transmission image (gray scale) of the array during fabrication, overlaid with UV-cured optical adhesive fluorescence (gray). (c) Scanning electron microscopy image of the completed array after acetone cleaning. (d) Simulated focus profile of the array where the origin is the lens focal spot, using a lens with a NA of 0.15 and Gaussian beam optics. The 125-μm lateral displacement between the focal zones is compensated by image realignment.

the middle 2/3 of the scans, which was approximately linear. Full fringe detection was obtained with a four-channel, 5-Msample/s, 12-bit analog-to-digital converter to simultaneously digitize the interference signals, which were balance detected, bandpass filtered, and software demodulated. A pair of doublet lenses (f = 80 mm, f/3.2) was used in the combined sample arm to form four focal spots with the array tip at 1:1 magnification. Axial scans from each channel covered 250 μm in depth, with 50% overlap between adjacent channels, reducing the detector bandwidth requirement from 1.4 to 0.7 MHz.[9] With no overlap this requirement could be further lowered to 350 kHz. The focal spot profiles of the array tip were measured with a beam profiler and compared with the calculated values. Figures 3(a) and 3(b) illustrate the 8-μm FWHM beam diameter of channel # 4 (in focus), while the other three channels show different degrees of defocusing. Figure 3(c) illustrates the calculated and measured FWHM beam diameter variations across the imaging depth. Although the beam of a single fiber rapidly defocused over the full imaging depth of ~500 μm, all the image data could be acquired within one Rayleigh length from the nearest focal spot by use of the four-channel array. The system was able to resolve 9-μm bars on a U.S. Air Force resolution target, as shown in Fig. 4(a). Finally, we acquired an OCT image of a tooth from a cadaver, as shown in Fig. 4(c). Corresponding well to the anatomy shown in Fig. 4(b), the surface of the tooth and the dentin–enamel interface were clearly visualized, with the latter resolved better than previously reported.[10]

The multifocus array tip allows a higher NA for each fiber, which improves the lateral resolution and increases the signal intensity. An N-channel tip also divides the axial scan depth by N for each channel, which allows a smaller detector bandwidth and (or) a higher RSOD frequency. The multichannel interferometer provides better power distribution along the imaging depth and reduces the required detector dynamic range. These advantages are critical for implementing real-time imaging, where the trade-offs among signal bandwidth, lateral resolution, depth of focus, and dynamic range have prevented video-rate imaging to date in cross-sectional ultrahigh-resolution OCT systems. Using an eight-channel array, one can achieve 2 μm (axial) × 5 μm (lateral) imaging resolution over

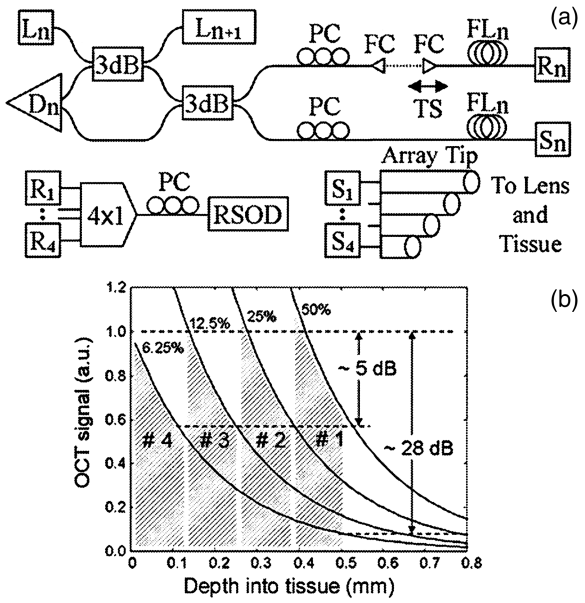

Fig. 2. (a) Schematic of the fiber-optic cascaded Michelson interferometer. TS, translation stage; FCs, fiber collimators; PCs, polarization controllers; L_n, D_n, FL_n, R_n, S_n: light source, detector, fiber loops, reference and sample arms of the nth cascade, respectively. (b) Calculated OCT signal levels (assuming tissue optical attenuation of 3.2 mm^{-1} and a collimated beam and ignoring coupling losses) with geometric power distribution in the four channels, illustrating better power utilization along the imaging depth. If a single channel is used to image the entire 500-μm depth, the required dynamic range is ~28 dB. This is reduced to ~5 dB when four channels are used with geometric power distribution.

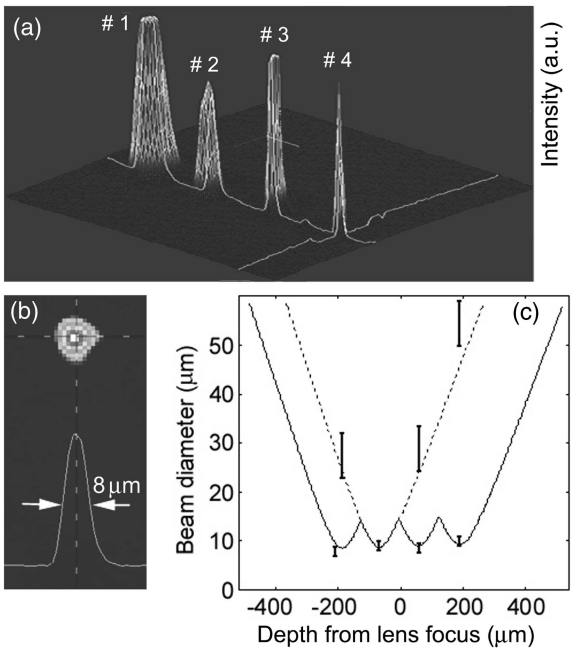

Fig. 3. (a) Measured beam profiles of the array in air when channel # 4 fiber is in focus (channel # 2 has excess loss as a result of coupling imperfection). (b) Focal spot detail of the fiber in focus. (c) Calculated (lines) and measured (bars) FWHM diameters of the array: single channel (dashed curve) and full array (solid curve). The error bars indicate variations of the beam diameter measured at orthogonal angles.

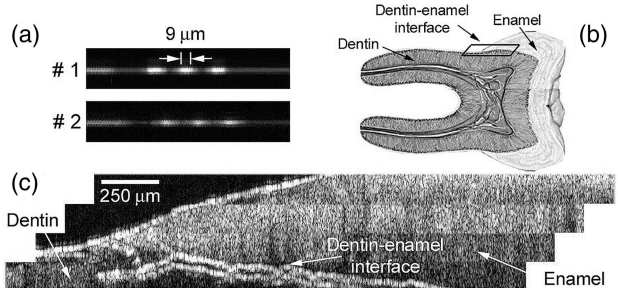

Fig. 4. (a) OCT images of resolution target (9-μm bars) acquired by channels # 1 (in focus) and # 2 (out of focus). (b) Anatomy of the human tooth (adapted from Ref. 11), with the small box indicating the dentin–enamel interface zone. (c) Fused image acquired from the four-channel OCT system of a tooth from a cadaver, clearly demonstrating the dentin–enamel interface. Intensity discrepancies between channels are due to image fusion imperfections.

an ~500-μm depth with existing photodetectors, since the required signal bandwidth is only 1.7 MHz for 32 frames/s and 500 lines/image. Finally, the array design presented here can be further improved and implemented for endoscopic applications. Because the size of the prototype array tip is small (500-μm width) and the lens diameter can be smaller than 5 mm without significant degradation of the array performance, a radial or linear scanning array tip can be fabricated to pass through the accessory channel of a large therapeutic endoscope for gastrointestinal imaging. A 2-mm-diameter probe is practical for use with standard endoscopes with smaller-diameter fibers and a custom-designed lens. In the future individual fiber tips on the array can also be angle polished to reduce backreflection and improve sensitivity. The obvious disadvantage of a multichannel OCT system is the increased system complexity. The improved image quality at a real-time frame rate may have a significant effect on endoscopic applications, especially in clinical ultrahigh-resolution systems for endoscopy.

In summary, we have reported a novel design and fabrication process of a multifocus fiber array tip, as well as the design of a cascaded multichannel interferometer for high-speed, high-NA OCT imaging.

This work was supported by the Natural Science and Engineering Research Council of Canada, the Canadian Institutes for Health Research, the Canadian Foundation for Innovation, Photonics Research Ontario, and St. Michael's Hospital. V. X. D. Yang (victor.yang@utoronto.ca) thanks Z. Chen, J. de Boer, and S. Yazdanfar for helpful discussions.

References

1. D. Huang, E. A. Swanson, C. P. Lin, J. S. Schuman, W. G. Stinson, W. Chang, M. R. Hee, T. Flotte, K. Gregory, C. A. Puliafito, and J. G. Fujimoto, Science **254,** 1178 (1991).
2. L. Vabre, A. Dubois, and A. C. Boccara, Opt. Lett. **27,** 530 (2002).
3. M. Laubscher, M. Ducros, B. Karamata, T. Lasser, and R. Salathé, Opt. Express **10,** 429 (2002), http://www.opticsexpress.org.
4. M. Akiba, K. P. Chan, and N. Tanno, Opt. Lett. **28,** 816 (2003).
5. J. M. Schmitt, S. L. Lee, and K. M. Yung, Opt. Commun. **142,** 203 (1997).
6. Y. Wang, Y. Zhao, J. S. Nelson, Z. Chen, and R. S. Windeler, Opt. Lett. **28,** 182 (2003).
7. W. Drexler, U. Morgner, F. X. Kartner, C. Pitris, S. A. Boppart, X. D. Li, E. P. Ippen, and J. G. Fujimoto, Opt. Lett. **24,** 1221 (1999).
8. B. Qi, P. A. Himmer, M. L. Gordon, V. X. D. Yang, D. L. Dickensheets, and I. A. Vitkin, Opt. Commun. **232,** 123 (2004).
9. V. X. D. Yang, M. L. Gordon, B. Qi, J. Pekar, S. Lo, E. Seng-Yue, A. Mok, B. C. Wilson, and I. A. Vitkin, Opt. Express **11,** 794 (2003), http://www.opticsexpress.org.
10. B. W. Colston, M. J. Everett, L. B. DaSilva, L. L. Otis, P. Stroeve, and H. Nathel, Appl. Opt. **37,** 3582 (1998).
11. F. Netter, *Atlas of Human Anatomy* (Icon Learning, Teeterboro, N.J., 1998).